Deep Mining 2014 – M Hudyma and Y Potvin (eds)

doi:10.36487/ACG_rep/1410_24_Vatcher

Mine-scale numerical modelling, seismicity and stresses at Kiirunavaara Mine, Sweden

J Vatcher *Luleå University of Technology, Sweden*

SD McKinnon *Queen's University, Canada*

J Sjöberg *Itasca Consultants AB, Sweden*

Abstract

LKAB's Kiirunavaara Mine, located in northern Sweden, has exhibited seismic behaviour since the mining production extended below 700 m depth. Iron ore is mined from the 4.5 km long orebody via sublevel caving at a production rate of 28 m t per annum. The deepest current production level is at approximately 800 m depth, and current mining plans call for mining to about 1,200 m depth. It is thus of critical importance for LKAB to gain a deeper understanding of the stress and rock mass behaviour at the mine.

The Kiirunavaara orebody has complex geometry and geology, which is represented using the discontinuum distinct element code 3DEC. As part of a larger series of models investigating the influence of strength and structural geology on rock mass behaviour, the results of multiple continuum models are presented. The goals of these continuum models included: (i) obtain a better understanding of the virgin stress field and redistribution of stresses caused by mining, (ii) further define the extent of mining induced plastic failure; and (iii) increase the understanding of existing failure mechanisms at the mine.

The elastic and plastic continuum models accurately produced principal stresses similar to measurements recently conducted at two sites in the mine, confirming the previously estimated virgin stress state. Spatial correlations between plastic failure in the model and seismicity in the hanging wall and footwall were found. However, these correlations were not consistent throughout either material for any evaluated set of material properties; either the plastic failure in the footwall or hanging wall corresponded well with seismicity. This may be because a set of rock mass properties which represent rock mass failure at this scale have not been evaluated or that some underlying failure mechanisms causing seismicity are not represented in the models, for example, failure along discontinuities. Some events larger than moment magnitude of 1.2 in the hanging wall, in particular shear source mechanisms events, do not correspond well with plastic failure from the model. These results potentially indicate that geological structures, which are not represented in these models, influence mine behaviour.

The improved understanding of input data, rock mass behaviour, and failure mechanisms as a result of these models has a direct impact upon mine excavation design and future rock behaviour investigations, and will be used in the continued research, as well as in mine planning.

1 Introduction

Since mining below approximately 700 m depth (Level 907 m), LKAB's Kiirunavaara Mine in northern Sweden has experienced mining induced seismicity and rockbursting. As mining progresses from the current main haulage level (Level 1045 m) to the next main haulage level (Level 1365 m), it is expected that the seismic behaviour at the mine will continue. Analysis of the mine's seismicity conducted at LKAB and Luleå University of Technology (LTU) (e.g. Dahnér et al. 2012; Skott 2013) has enhanced the understanding of the mine's behaviour. However, the direct correlation between geology, rock mass properties and failure mechanisms remains largely unknown. Developing a greater understanding of the underlying causes of the failure mechanisms of the rock mass is critical for continued safe production at the mine.

The Kiirunavaara Mine uses sublevel caving to extract 28 m t of magnetite ore per annum. The orebody is approximately 4.5 km long, with variations in thickness (metres to greater than 150 m) and dip (50-70°).

Considerably less dense and stiffer than the ore, the host rock is comprised of trachyte in the footwall, and rhyodacites in the hanging wall. Alterations and geological structures, in the forms of discontinuities (fractures and faults) and dykes, exist throughout the host and ore materials.

The large scale failure mechanisms at the Kiirunavaara Mine in three-dimensions (3D) have not been previously explored; prior to the work presented in this paper, only elastic numerical stress analysis of the mine existed in 3D. Plastic analysis enables a direct comparison of the plastic damage zone in the model to seismicity measured at the mine (e.g. Andrieux et al. 2008). This comparison will improve the understanding of the extent of the seismically active plastic damage zone, the influence of geology on rock mass failure mechanisms, and the calibration of material properties. In addition, a recent stress measurement campaign involving measurements at two deep levels in the mine, as described by Ask (2013), provides an opportunity to evaluate the previously determined virgin stress state at the mine (Sandström 2003), the redistribution of stresses caused by mining, and the influence of material properties upon this stress redistribution.

The objectives of this analysis are:

- Evaluate the validity of the virgin stress field as calculated by Sandström (2003).
- Provide further understanding of the redistribution of stresses at the mine.
- Increase the understanding of the extent of the plastic damage zone and the possible correlation to the seismogenic zone at depth.
- Identify seismic events anomalous to continuum behaviour, thereby directing future discontinuum analyses and investigations of mine geology.

2 Methodology and model setup

2.1 Methodology

These models are part of a project to investigate the underlying causes of seismicity at the Kiirunavaara Mine (see Vatcher et al. (2014) for a description of the overall project). The focus is upon a selected study volume corresponding to a production region in the mine, named Block 33/Block 34. The study volume, located in the middle of the mine extending from surface to below the planned depth of the mine (Figure 1), was selected as it is one of the most seismically hazardous blocks in the mine. Instrumentation and measurement campaigns are focused inside of Block 33/Block 34, with the intention of developing modelling and supporting data acquisition procedures which can be repeated efficiently for other areas in the mine.

Due to the interest of incorporating geological structures, such as faults, in future models, the three-dimensional distinct element code 3DEC (Itasca Consulting Group, Inc. 2013a) was selected for the modelling. This paper presents the results of the mine scale models prior to the addition of discontinuities. These continuum models are the first steps to evaluating the influence of rock mass strength and geological structures on mine behaviour. Subsequent work will include adding large-scale discontinuities into the model.

Three continuum models were created to evaluate the influence of elastic or plastic materials and the footwall strength on stresses and rock mass behaviour (Table 1). Due to the large scale of the models, development excavations were not represented. An explicit excavation sequence was not used in these models; a single excavation stage removed all stopes from the beginning of underground mining to the present day production levels (see Figure 1 for current production levels along the length of the mine). The production sequence was simplified according to sublevel and production area along the strike of the orebody. Caving in the orebody was simulated as a void with no extension into the hanging wall.

Table 1 Model cases

Case	Constitutive model	Footwall strength case	Excavation sequence
A	Elastic, isotropic	Base strength	All stopes excavated simultaneously
B	Perfectly plastic, isotropic	Base strength	All stopes excavated simultaneously
C	Perfectly plastic, isotropic	Low strength	All stopes excavated simultaneously

Using Rhino (Robert McNeel & Associates 2014) and KUBRIX (Itasca Consulting Group, Inc. 2013b), a mesh of the geomechanically relevant geological, physical and user-defined boundaries was created for blocks in 3DEC. This model generation technique enabled more complex geometries to be created than previously possible with other techniques and has the additional benefits of adaptable discretisation and the ability to easily change the model scale of interest. The model geometry was developed so that more geometric detail exists in Block 33/Block 34 (Figure 1). Since regions external to the study block are represented in a more simplified manner, model results external to Block 33/Block 34 have a lower accuracy and resolution.

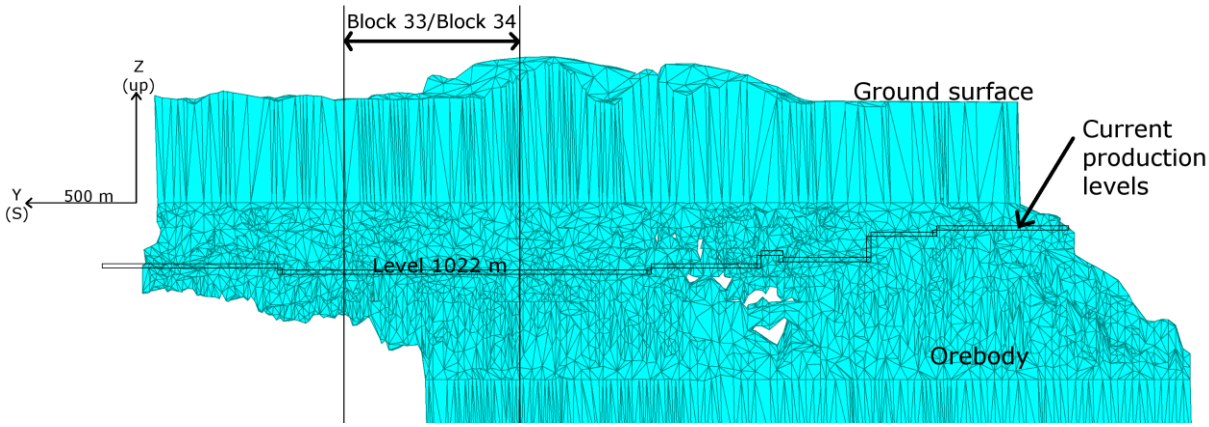

Figure 1 Simplified orebody geometry for 3DEC models, longitudinal section as seen from the hanging wall

2.2 Model setup

A distinction was made between the hanging wall, footwall and orebody, as these are the geomechanical domains of importance at this scale of continuum modelling. Material properties, listed in Table 2, were assigned based on information modified from Sjöberg et al. (2012). Base material properties (Case A and Case B) represent the best current estimate of the large scale rock mass strength parameters. The material properties used for the low strength footwall material (Case C) were selected as the lowest likely strength properties of the footwall material as described by Sjöberg et al. (2012). The footwall strength was reduced in this evaluation due to the result from Cases A and B.

Table 2 Material properties (from Sjöberg et al. 2012)

Property	Footwall base strength	Footwall low strength	Orebody	Hanging wall
Young's Modulus, E	70 GPa	70 GPa	65 GPa	70 GPa
Poisson's Ratio, v	0.27	0.27	0.25	0.22
Density, ρ,	2,800 kg/m^3	2,800 kg/m^3	4,700 kg/m^3	2,700 kg/m^3
Cohesive strength, C	10.2 MPa	4.9 MPa	6.88 MPa	6.68 MPa
Tensile strength, T	2.23 MPa	0.21 MPa	1.21 MPa	1.00 MPa

Friction angle, ϕ	58.2°	49.5°	54.3°	55.1°

Model discretisation was dependent upon location relative to Block 33/Block 34 and the orebody; the densest discretisation was in the study volume. In the remaining volume of the orebody and volume immediately surrounding the orebody, the discretisation was slightly coarser. In the remaining host rock to the boundaries of the models, discretisation increased further in coarseness. Model boundaries were extended in depth, width and length (Figure 2). The boundary representing the physical ground surface remained unconstrained and zero normal displacement conditions were applied to the remaining boundaries.

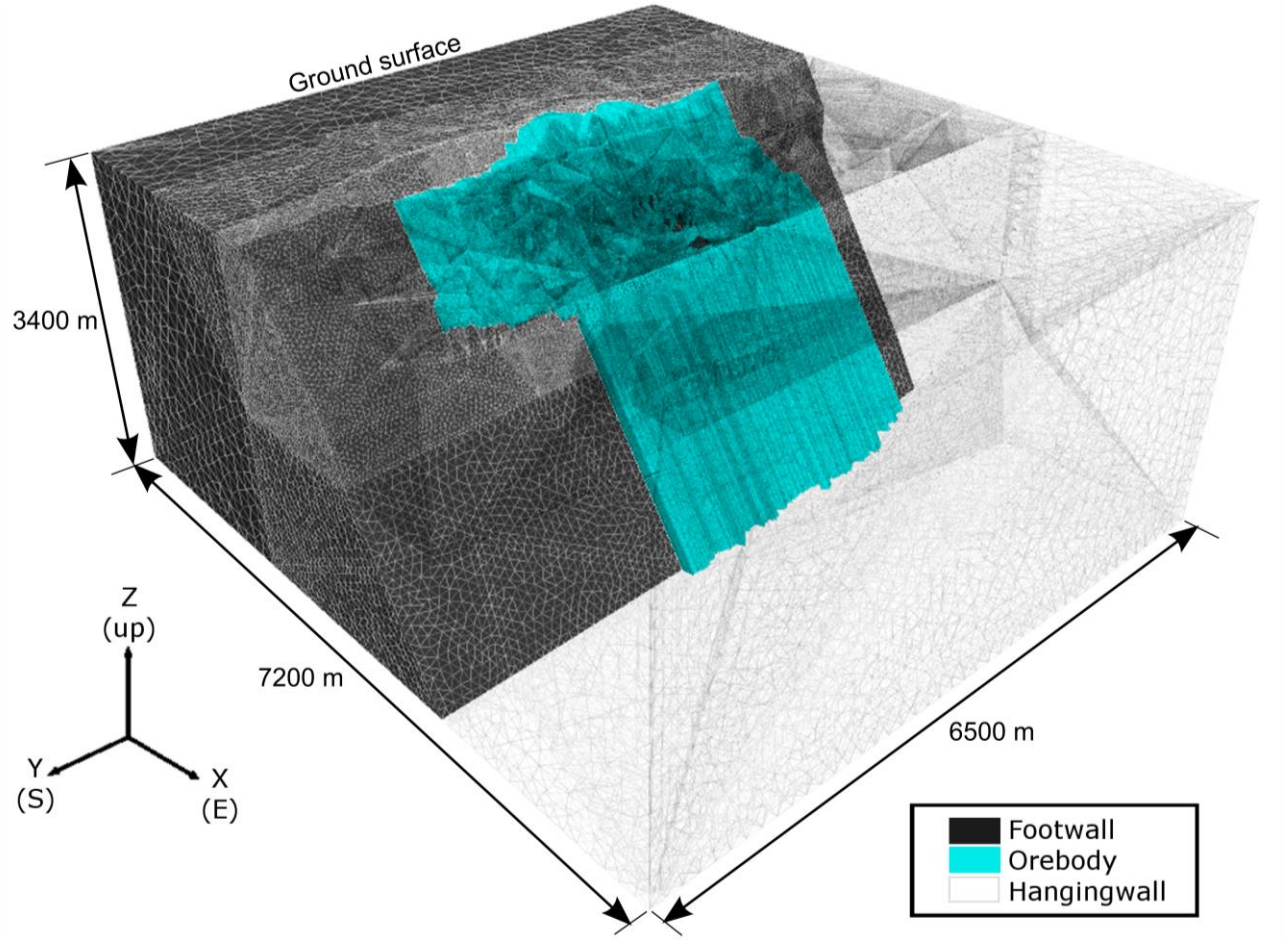

Figure 2 Isometric view of 3DEC model

Sandström (2003) evaluated historic stress measurements at the mine to determine relationships describing the virgin stress state according to depth. These relationships, as listed in Equations (1) through (3), were used in conjunction with gravitational loading to create the stress field prior to mining in the models. Due to variable topography, the vertical datum was selected as the highest point in the current topographic map to eliminate tensile stresses below the ground surface prior to mining. All stresses at the datum are zero, below the datum are compressive and above the datum are tensile (refer to Equations (1) through (3)). A selection of any alternative point as the vertical datum would result in in situ stresses that were tensile in the model, which is not representative of the virgin stress state in the rock mass.

$$\sigma_{ew} = 0.037z \quad (1)$$

$$\sigma_v = 0.029z \quad (2)$$

$$\sigma_{ns} = 0.028z \quad (3)$$

Where:

z = depth below surface, m.

σ_{ew} = stress in east–west (x axis) direction (Kiirunavaara underground coordinate system), MPa.

σ_v = stress in vertical (z axis)direction (Kiirunavaara underground coordinate system), MPa.

σ_{ns} = stress in north–south (y axis) direction (Kiirunavaara underground coordinate system), MPa.

2.3 Evaluation criteria

Stresses from all model cases and areas of yielded material from the plastic model were compared to measured data regarding the rock mass behaviour and stress regime at the mine. The measured data included:

- Results from recent stress measurements at two locations in the mine (Ask 2013).
- Seismicity at the mine as measured by the seismic monitoring network.

As described by Ask (2013), multiple overcoring measurements using the Borre probe were made at each of the measurement sites to obtain the absolute stresses. The measurement sites, at Level 1165 m and Level 1252 m, were located approximately 100 and 200 m deeper than any measurement used by Sandström (2003). Both measurement sites were inside of the study area.

The seismic data used for this analysis consisted of all events recorded at the mine since the installation of the mine-wide seismic network system in 2008 (see Dahnér et al. (2012) for a description of the seismic network and its installation). Location, seismic moment, S-wave energy and P-wave energy were automatically determined by the system. For purposes of this analysis, data was filtered so that all events were within Block33/Block 34. Data was not filtered based on time, since the mine volume was excavated in a single step in the plastic model.

The seismic data used in this analysis was not filtered based on the location accuracy; however, statistics provided from the seismic network system regarding event location accuracy are presented for evaluated datasets. Events occurring outside of the volume of good seismic network coverage have less accurate information, including location and magnitude. Extensive seismic network coverage exists in the footwall and orebody at depth, with less coverage at depth in the hanging wall, and poor coverage near surface. Future work will add event accuracy filtering to the analysis.

3 Results and discussion

3.1 Stresses

The principal stress magnitude and orientation results from Cases A, B and C are compared to the measured principal stresses in Figures 3 and 4 for the measurement sites at Level 1165 m and Level 1252 m respectively. In general, the results from all models compare very well with the stress measurements.

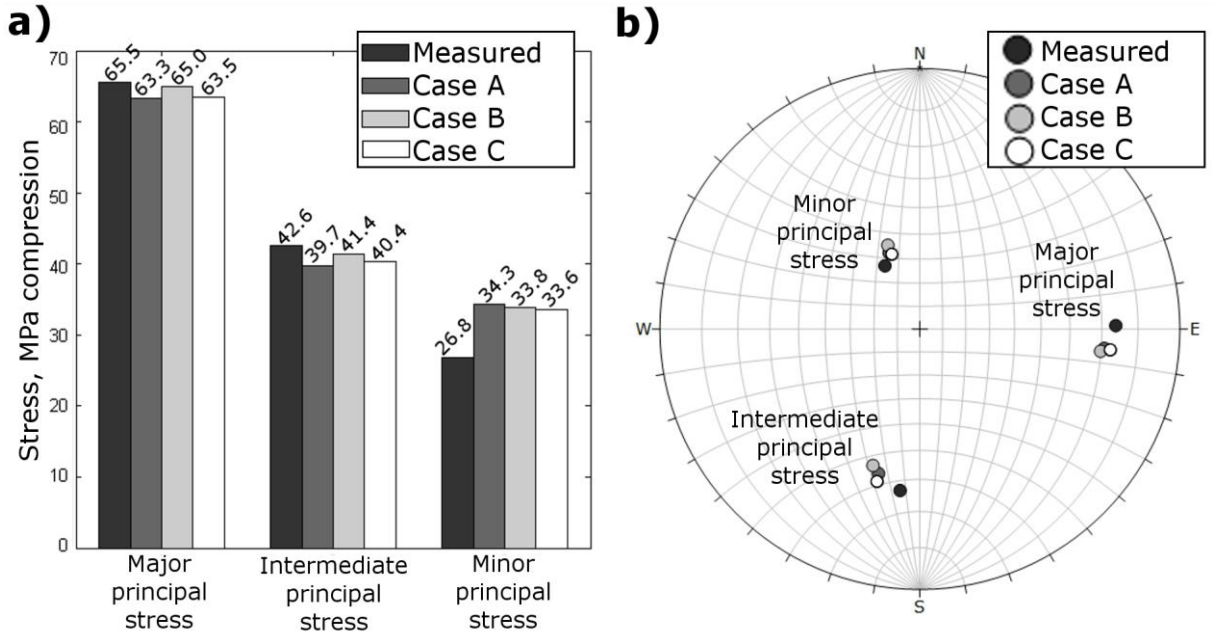

Figure 3 (a) magnitudes; and (b) orientations of principal stresses from the models and measurements at the Level 1165 m measurement site. Orientations are presented in mine coordinates, where east is aligned with the positive x axis

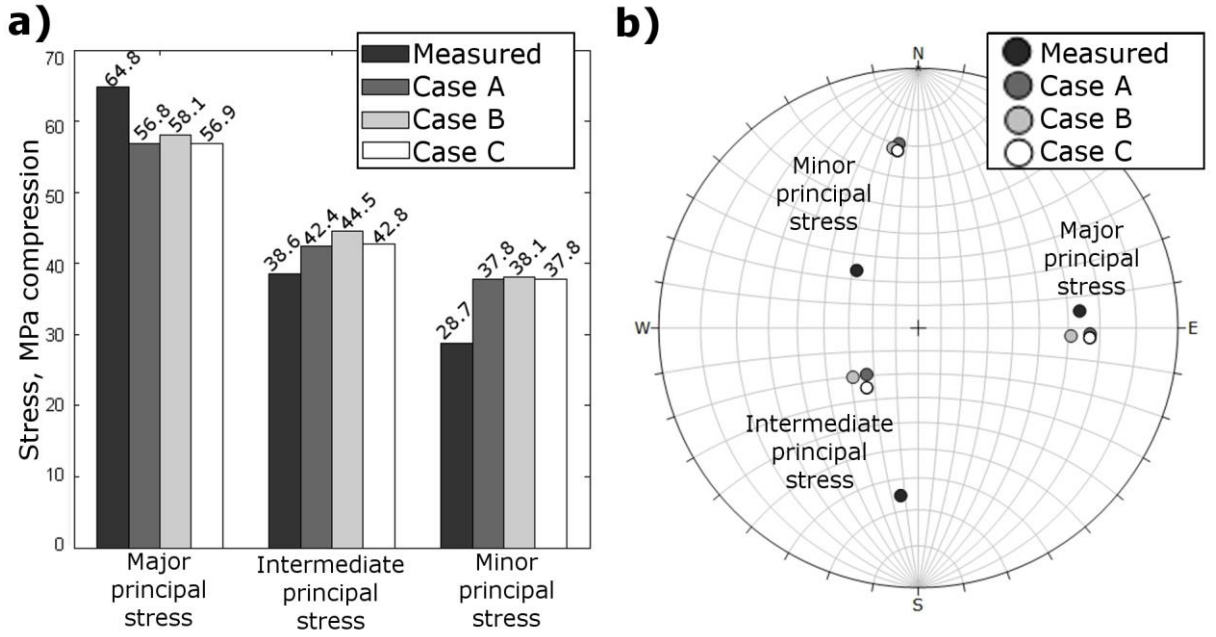

Figure 4 (a) magnitudes; and (b) orientations of principal stresses from the models and measurements at the Level 1252 m measurement site. Orientations are presented in mine coordinates, where east is aligned with the positive x axis

Results from the models and measurements at the Level 1165 m measurement site were very consistent in magnitude and direction for all principal stresses (Figure 3). All models resulted in minor principal stresses that were of larger magnitude than those measured at Level 1165 m. At this measurement site, the use of elastic or perfectly plastic materials had little impact upon the resulting principal stress magnitudes or orientations. The stress state was not very sensitive to the reduction of footwall strength.

The model and measurement results at the Level 1252 m site also agreed very well, although they had a larger variation in both magnitude and orientation than at the previous measurement site (Figure 4). All models and the measurements resulted in similar directions of the major principal stresses, however there are some discrepancies for directions of the intermediate and minor principal stresses at this site. Similar to the measurement site at Level 1165 m, the models resulted in a higher magnitude minor principal stress than what was measured. The use of perfectly plastic materials had very little influence upon the resulting principal stress magnitudes and directions in the models.

The general concurrence between the model results and the measured stresses confirms that the virgin stress state as defined by Sandström (2003), which was based on measurements at shallower depth, appears to be consistent with depth. In addition, these models have confirmed that, at this scale, the use of elastic or plastic materials with simultaneous excavation has little impact upon the resulting stresses. The reduction in footwall strength had little impact upon the stress state at either site.

Further investigation is required to ascertain:

1. Why the magnitude of minor principal stress from the models is consistently lower than those measured.
2. Why the results from the models and the measurements of intermediate and minor principal stress directions have a larger difference at the Level 1252 m site.

Possible explanations for these results include coarse model zoning, model geometry oversimplifications (in the form of geomechanical units or sequence), and/or geological structures in the mine (and absent in the model) causing a rotation of the stress field.

3.2 Plastic failure zone and seismicity

Plastic failure was evident in the hanging wall, footwall, and directly under the active level in the orebody. See Figure 5 for plastic failure from Case B along an example plane in Block 33/Block 34. Plastic failure in the orebody and footwall does not extend very far from the mining excavation. However, as seen in Figure 5, the plastic failure extends much further into the hanging wall. Near surface, it is likely that the model overestimates the extent of the plastic damage zone of the rock mass because this model was not designed to evaluate rock mass behaviour in this area. The discretisation was coarse, tensile failure existed at an early stage in the model near surface, and caving mechanisms, which would directly influence the extent of the plastic damage zone at surface, were not explicitly represented in the models. Furthermore, although subsidence and tension cracks exist on surface, there has been no evidence of such rock mass failure extending as far as seen in the model. Near the lowest production level, the plastic failure more likely represents the actual extent of rock mass yielding. As such, the analysis in this section progresses with a focus on the plastic damage zone at depth.

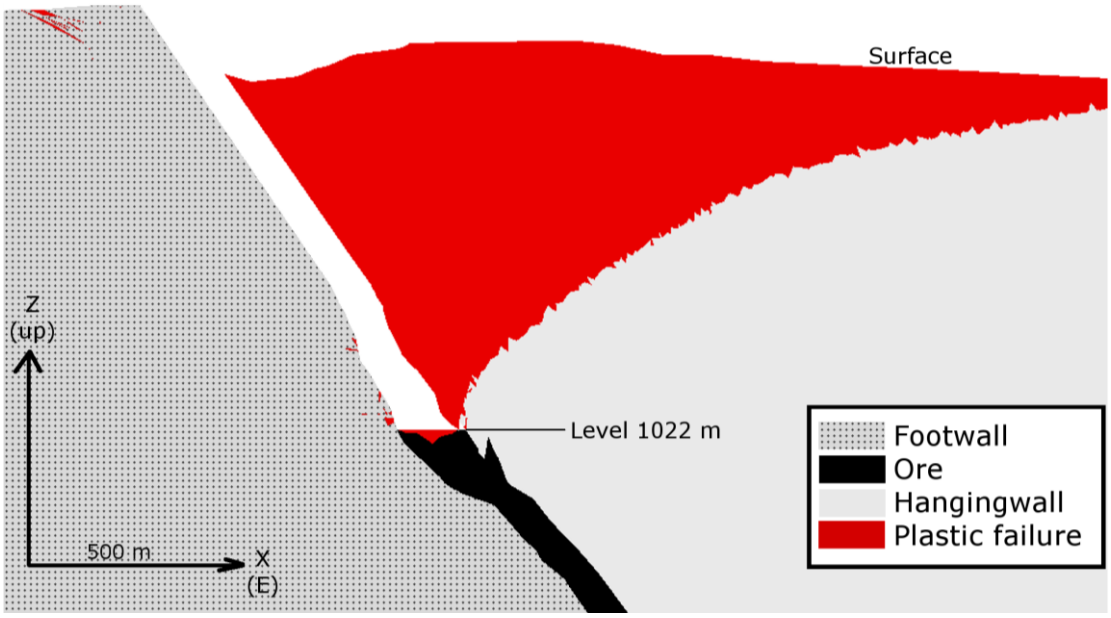

Figure 5 Plastic failure from Case B along a vertical slice through the study area; approximately perpendicular to the strike of the orebody

Rock mass failure mechanism, event source type and magnitude are closely linked. To better understand the seismic behaviour at the mine, the ratio of the S-wave energy to the P-wave energy (Es/Ep) was used to filter seismic events into tensile events (Es/Ep<3), mixed source events (3≤Es/Ep≤8), and shear events (Es/Ep>8). For guidelines, see ISS International (2006). The moment magnitude, which is different from the local magnitude calculated at the Kiirunavaara Mine, was calculated from measured moment energy using the Hanks–Kanamori equation (Hanks & Kanamori 1979):

$$m_M = \frac{2}{3} logM - 6.1 \tag{4}$$

Where:

m_M = moment magnitude.

M = seismic moment, Nm.

Figure 6 presents a histogram showing the spread of moment magnitudes categorised by event source type for all recorded events in the study area at the Kiirunavaara Mine. Since the installation of the seismic system at the mine, 67% of the events have been of a shear nature, 22% had a mixed source, and 11% were tensile. However, the events which have a tensile source mechanism have a slightly higher average magnitude.

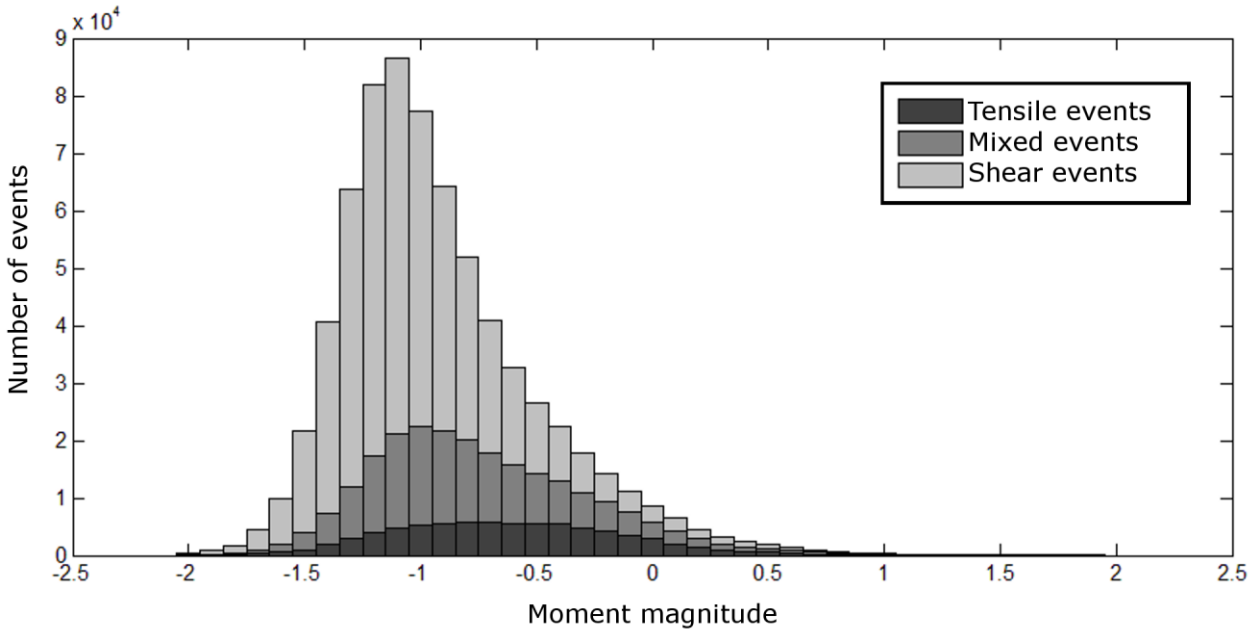

Figure 6 Histogram of moment magnitude by event source type

The location error residuals for all events in the study area were, on average, smaller than that of the maximum model zone sized in Block 33/Block 34 (Figure 7). This indicates that the locations of seismic events and the locations of plastic failure in the model are compatible for comparison purposes.

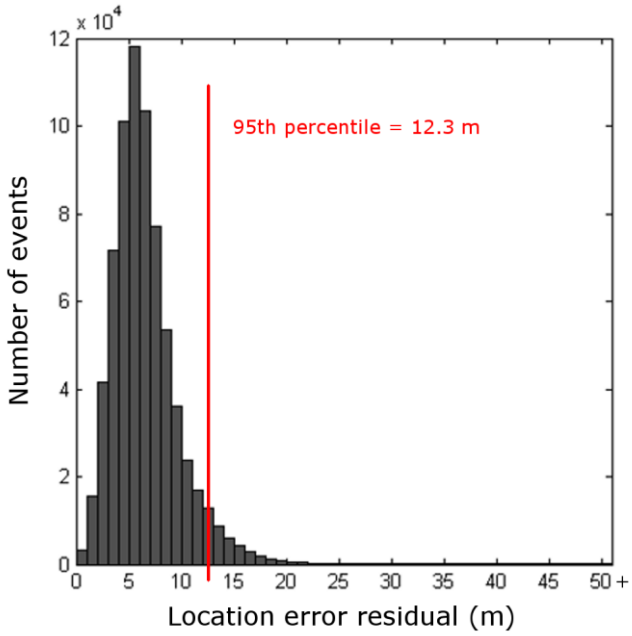

Figure 7 Histogram of location error residual for all seismic events in the study area

When considering all magnitudes of events in the mine's entire seismic catalogue, there were no obvious spatial differences between events of different source mechanisms. However, spatial clustering was observed. One such cluster is shown in Figure 8, illustrating all events in Block 33/Block 34 since the installation of the seismic system. In the hanging wall, the boundary of the seismogenic zone has a distinct arced shape, starting near the current mining level and extending upwards and outwards into the hanging wall. It is important to consider that the seismic network coverage in the hanging wall is not as extensive as in the footwall, so some of these events have lower location and magnitude accuracy.

The shape of the hanging wall cluster in Figure 8 was mirrored by the shape of the plastic failure zone from Case B (Figure 8(a)). Most of the events in the hanging wall were located inside of the plastic failure zone. With the time scale used in this analysis, there was no indication that the events inside the model's plastic failure zone were biased towards a particular source mechanism. Despite using the same material properties for the hanging wall, the plastic failure in Case C did not correspond well to the seismic cluster in the hanging wall (Figure 8(b)). The footwall strength influenced the extent of plastic failure in the hanging wall. The strong correlation between the seismicity and the plastic failure from Case B provided a preliminary indication that the base rock mass parameters used were representative.

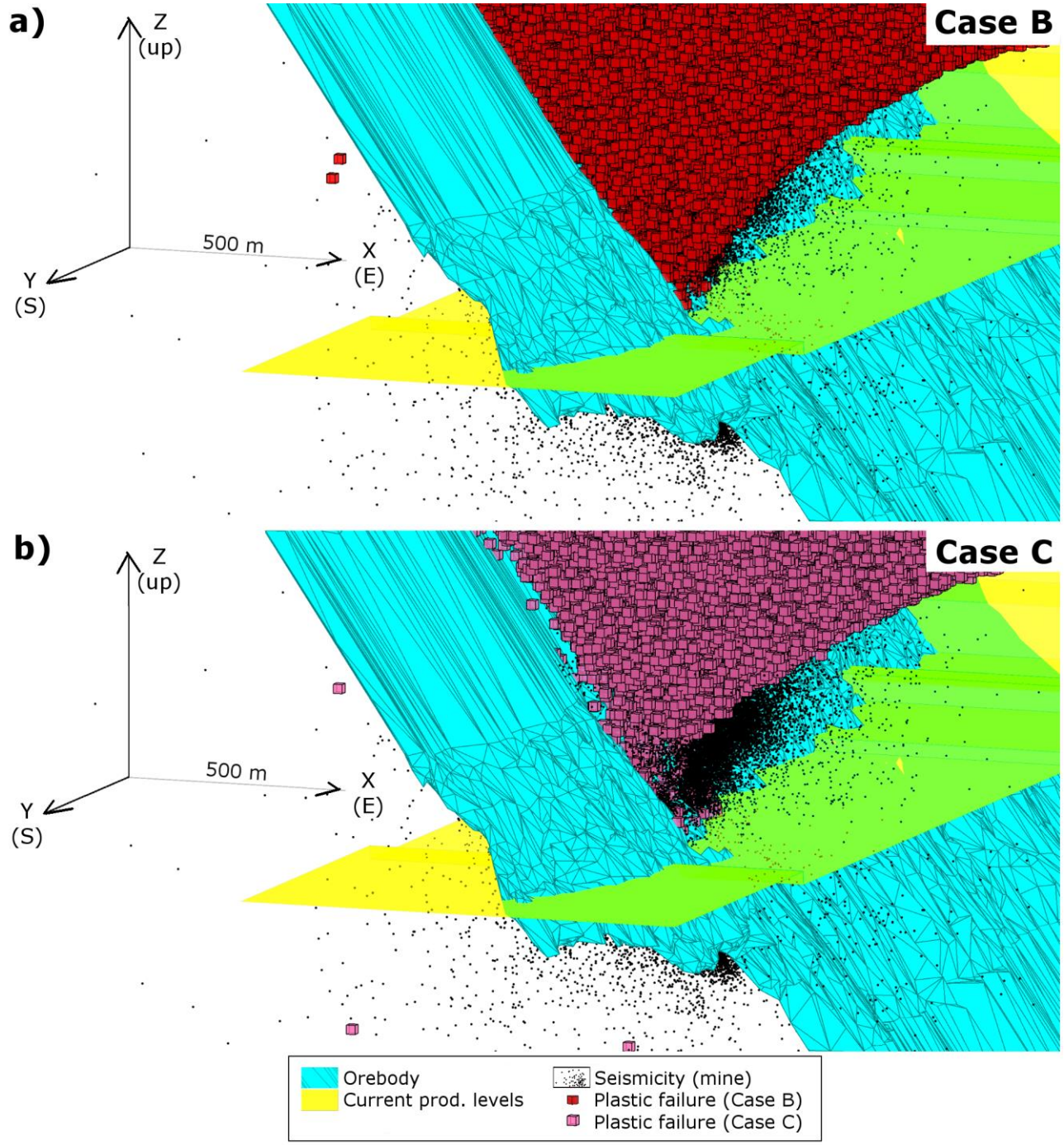

Figure 8 All seismic events in the study area since the installation of the seismic system with plastic failure from the model overlaid as seen from the hanging wall for (a) Case B; and (b) Case C

However, the comparison of plastic failure and seismicity in the footwall did not indicate that the base material properties were representative of the large scale rock mass behaviour. The plastic failure in the footwall from the case with the base material properties (Case B) did not correspond well to the seismic behaviour in the mine (Figure 9(a)). The long clusters of seismicity dipping towards the orebody under the active mining level in Figure 9 are orepass noise and not related to rock mass behaviour. Case B did not show as much failure as is evident in the seismicity, which may indicate that the footwall material properties were too strong. Upon reduction of the footwall strength (Case C), there was more correlation between the plastic failure and seismicity (Figure 9(b)). The contradictory results regarding footwall strength when comparing the plastic failure in the hanging wall and the footwall to seismicity may indicate that a representative combination of material properties has not yet been determined or that additional failure mechanisms not incorporated in this model (such as failure along discontinuities or anisotropy) are responsible for some of the seismicity at the mine.

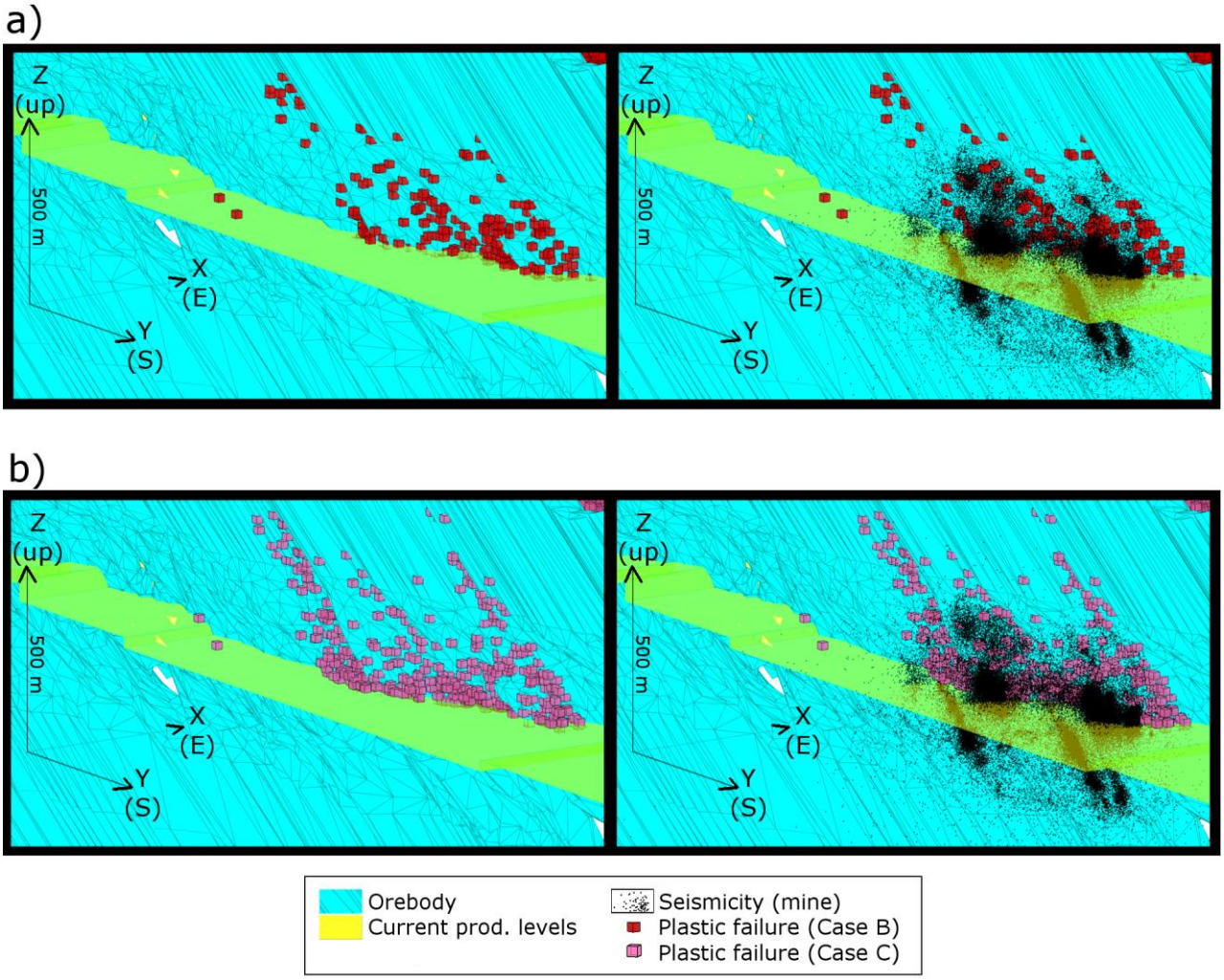

Figure 9 Plastic failure in the footwall (left) with all seismic events in Block 33/Block 34 from the catalog overlaid (right) for (a) Case B; and (b) Case C

Seismic events were also filtered based on moment magnitude. Events larger than a moment magnitude of 1.2 were considered for this analysis because large magnitude events are of interest from a damage perspective. This magnitude was selected as it significantly reduced the number of events to analyse (as illustrated in the histogram presented in Figure 6). Figure 10 provides statistics regarding the large magnitude event data. Shear events still dominate as the prominent source mechanism for all moment magnitudes above 1.2.

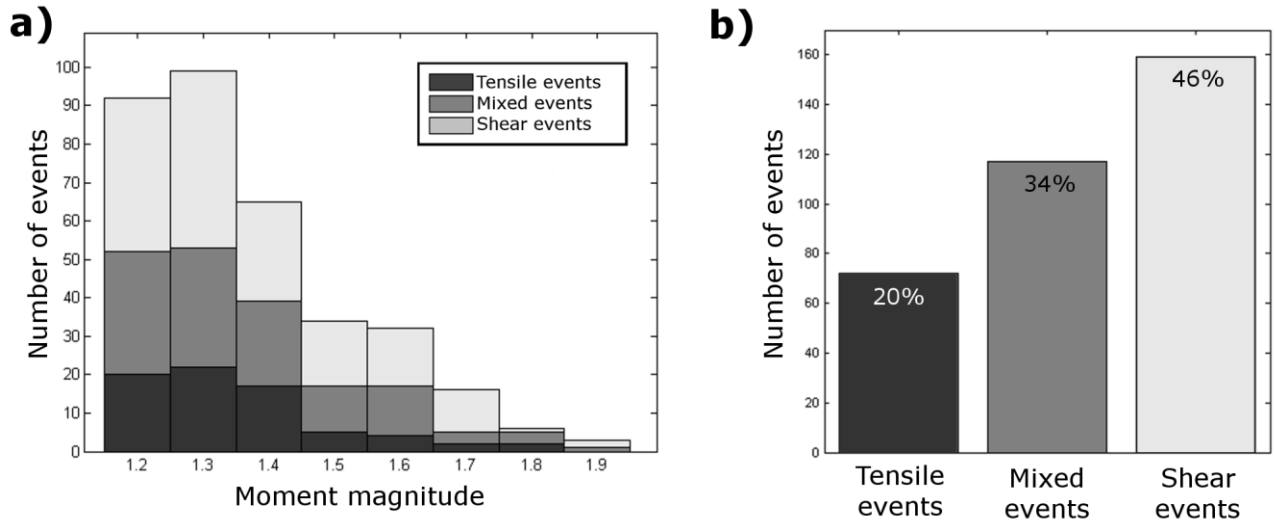

Figure 10 (a) histogram of magnitude by event source type for events larger than moment magnitude 1.2; (b) histogram of event source type for events larger than moment magnitude 1.2

When considering events with a moment magnitude greater than 1.2, the location of the majority of events is still statistically comparable to the model based on event location error and zone size (Figure 11). Although the distribution of location error residuals has a different shape than the distribution when considering all events in the study area, the mean location error residual is less than the maximum zone size in the study area.

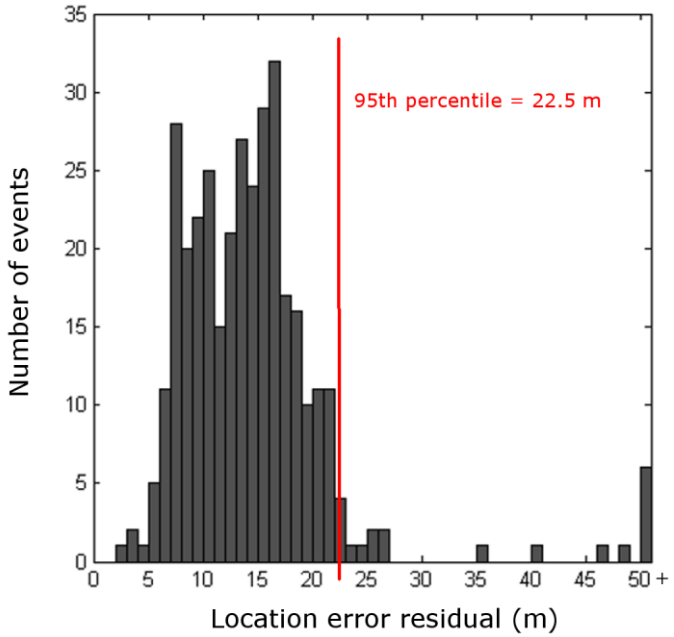

Figure 11 Histogram of location error residual for all events in the study area with moment magnitude larger than 1.2

Interestingly, the seismic events of moment magnitude greater than 1.2 for all source types create distinct clusters in the hanging wall (Figure 12(a)). Events from this set that have a shear source mechanism are shown in Figure 12(a) as cubes. Upon examination of this subset of events, it is clear that large magnitude shear events are not spatially part of the clusters created by the other types of large magnitude events. Once volumes of plastic failure from Case B is overlaid in Figure 12(b). Case B was selected as this was the case with the best correspondence between failure and seismicity in the hanging wall. Two significant

observations can be made. Firstly, the large magnitude events do not necessarily fit well inside of the model's plastic failure zone, in particular in the north end of the study area. This is likely caused by an oversimplification of geomechanical unit geometry, or the assumption of a geological continuum within the model. The second observation is that many of the large shear type events are outside of the model's plastic failure zone. These models do not provide conclusive evidence indicating whether these events are part of the hanging wall caving failure mechanism, fault slip events or if they have inaccurate locations due to the limitations of the seismic system.

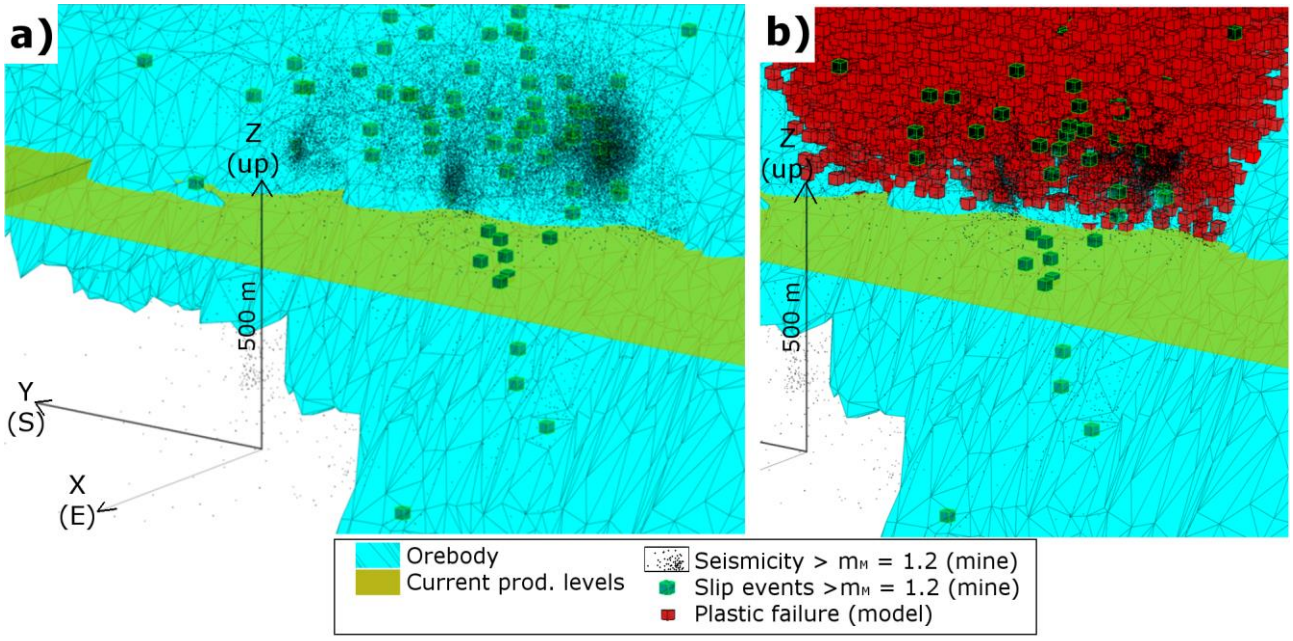

Figure 12 (a) seismic events in the hanging wall with a moment magnitude greater than 1.2; (b) with plastic failure from Case B overlaid

4 Conclusions and recommendations

The following list outlines conclusions from this work:

- The results from the developed models correspond well with those of the recent stress measurement campaign. This implies that these 3D continuum models can reasonable predict large scale stress redistribution at the mine.
- The virgin stress state at the mine as previously defined by Sandström (2003) is consistent at depth.
- Using a simultaneous excavation sequence, elastic or perfectly plastic materials cause little impact upon the stress results for this specific case. In addition, the stress state at the measurement sites is not sensitive to a reduction in footwall strength.
- Plastic damage from the models corresponds well with the seismic event locations in the hanging wall or the footwall, dependent upon the footwall strength. This may indicate that a set of material properties to represent the large scale continuum behaviour has not yet been evaluated, or that the underlying failure mechanisms of some events were not captured in the models (such as discontinuum behaviour).
- There are some large magnitude shear events in the hanging wall that do not correspond with the plastic damage zone from the models. It is not clear if this is related to the caving mechanism or to geological structures. Interpretation of mechanisms in this region may not be reliable due to source location accuracy of events in the lower hanging wall region.

The following suggestions for future work are offered:

- Evaluate if a sequenced excavation will influence the resulting stresses at the mine site.
- Evaluate if smaller zone size in and surrounding the study area has any impact upon the elastic and/or plastic results.
- Evaluate the influence of how caving is represented in the models.
- Further evaluate the sensitivity of the models to changes in material properties and further define any additional geomechanical domains.
- Complete a more detailed, quantitative analysis of plastic failure versus seismicity. This includes using a model that has smaller time spans between excavations since the installation of the seismic system. In this way events can also be filtered based on time. Additional work is recommended regarding filtering events based on location accuracy.
- Evaluate the influence of including discontinuities.

Acknowledgement

The authors express extreme gratitude for the countless hours of assistance in the form of data acquisition and associated discussions from many individuals, including Christina Dahnér, Henrikki Rutanen, Mirjana Bošković, Stina Hallinder, Karin Lindgren, and Ulf B Andersson, at LKAB, and Daniel Ask at Pyöry AB. The authors also thank Jimmy Töyra (LKAB) for his thought provoking and prompt review of this manuscript. The input of the two anonymous reviewers was greatly appreciated. The authors are grateful to LKAB for providing this research opportunity via numerous resources, including the Hjalmar Lundbohm Research Centre.

References

Andrieux, PP, Hudyma, MR, O'Connor, CP, Li, H, Cotesta, L & Brummer, R 2008, 'Calibration of large-scale three-dimensional non-linear numerical models of underground mines using microseismic data', *Continuum and Distinct Element Numerical Modeling in Geo-Engineering*, no. 07-04.

Ask, D 2013, *Bergspänningsmätningar med Borre och spänningsmonitering med CSIRO HID i block 34, nivå KUJ1070, KUJ1165, och KUJ1252*, Pöyry internal report (in Swedish), no. 8H50124.130 Pöyry, Vantaa.

Dahnér, C, Malmgren, L & Bošković, M 2012, 'Transition from a non-seismic mine to a seismically active mine: Kiirunavaara Mine', *Proceedings of Rock Engineering and Technology for Sustainable Underground Construction: EUROCK 2012*, International Society for Rock Mechanics, Lisboa.

Hanks, TC & Kanamori, H 1979, 'A moment magnitude scale', *Journal of Geophysical Research*, vol. 84, no. B5, pp. 2348-2350.

ISS International 2006, *Glossary of terms used in routine mine seismology,* internal report, no. REP-GLOS-001r0, ISS International, Sydney.

Itasca Consulting Group, Inc. 2013a, *3DEC: Three-Dimensional Distinct Element Code*, version 5, Itasca Consulting Group, Inc. Minneapolis, http://www.itascacg.com/software/3dec

Itasca Consulting Group, Inc. 2013b, *KUBRIX*, Itasca Consulting Group, Inc. Minneapolis, http://www.itascacg.com/software/kubrix-geo

Robert McNeel & Associates 2014, *Rhino*, version 5, Seattle, Robert McNeel & Associates, http://www.rhino3d.com

Sandström, D 2003, *Analysis of the virgin state of stress at the Kiirunavaara mine*, Licentiate thesis, no. 2003:02, Luleå University of Technology, Luleå.

Sjöberg, J, Perman, F, Quinteriro, C, Malmgren, L, Dahnér-Lindkvist, C & Boskovic, M 2012, 'Numerical analysis of alternative mining sequences to minimise potential for fault slip rockbursting,' *Mining Technology*, vol. 121, no. 4, pp. 226-235.

Skott, J 2013, *Focal Mechanisms and Seismic Moment Tensors of Seismic Events in Kirunavaara Mine (Methodological- and Practical Aspects),* master's thesis, Luleå University of Technology, Luleå, no. 2013-75327629, viewed 7 April 2014, http://pure.ltu.se/portal/en/studentthesis/fokala-mekanismer-och-seismiska-moment-tensorer-av-seismiska-handelser-i-kirunavaaragruvan-metodologiska-och-praktiska-aspekter(cc83a95d-ff84-4fc6-8b50-2bac4506e3f3).html.

Vatcher, J, McKinnon, S & Sjöberg, J 2014, 'Modelling methodology: structural geology and rock mass behaviour at Kiirunavaara Mine', in R Alejano (ed.), *Proceedings of Rock Engineering and Technology for Sustainable Underground Construction: EUROCK 2014*, CRC Press, Boca Raton, pp. 643-648.